Photocurrent Imaging of the Layers Formed during the Electrooxidation of Gold

R. S. Hutton and D. E. Williams*

Contribution from the Department of Chemistry, University College London, 20 Gordon Street, London, WC1H 0AJ, U.K.

*Received November 15, 1993**

Abstract: A scanning laser electrochemical microscope was used to study localized photocurrents during the electrooxidation of gold. Images obtained solely with the supporting electrolyte suggested that the oxide layer is virtually homogenous. However in the presence of ferrocyanide a spectacular contrast was observed. A number of possible sources of image contrast are discussed and in part differentiated. In the presence of ferrocyanide the main mechanism for photoinduced current variations at a gold electrode is the effect of the small temperature change induced by the illumination on the rate of electrooxidation of Fe(II). The origin of the chemical heterogeneity thereby revealed was explored by examining the influence of electrode potential and pretreatment and is ascribed to a chemical species formed below regular monolayer oxide formation. Significantly this "incipient oxide" was found to be exceptionally stable, affecting image contrast up to oxygen evolution, and only being removed by prolonged evolution of hydrogen. Intense illumination resulted in a photoinduced aging or reconstruction of the oxide layer.

Introduction

An understanding of the origin of surface heterogeneity in electrochemical reactions is of considerable interest. Recently a variety of techniques have been developed which enable lateral variations in surface properties to be investigated.[1-7] In particular scanning laser photoelectrochemical microscopy (SCALPEM) techniques[7] implementing the photothermal,[8] photovoltage,[7] and photocurrent[6,7,9,11] responses at a variety of electrode materials have been presented. Images have provided important knowledge into phenomena such as the spatial distribution of kinetic control at disc electrodes,[8] the dissolution and reaction of sulfide inclusions in stainless steel,[9] heterogeneity at silicon[6] and passive metal[7] electrodes, and the origin of photoelectrochemical heterogeneity at the GaAs/electrolyte interface.[10,11]

The resulting images are inherently complex. They are images of the function of the electrode rather than its topography, although effects are seen as a consequence of multiple scattering of the incident light. Photocurrent image contrast at semiconducting and oxidized metal electrodes may arise from a variety of factors such as changes in "semiconducting" film thickness, minority carrier diffusion length, absorption coefficient, band-bending, light scattering and local composition as well as surface recombination effects associated with crystal imperfections.

In a previous publication[8] a more general variant was demonstrated which utilized the thermal effect on the current for an electrochemical process as the source of image contrast, essentially a scanning temperature jump experiment. The photothermal response was shown to be sensitive to electron-transfer kinetics, thus enabling spatial variations in kinetic and diffusion control to be determined, demonstrating the important influence of edge effects and surface relief on the current distribution at a disc electrode. It has been postulated that at a metallic electrode a photoinduced current may arise from photoelectron[12] and photohole emission.[13] However, during photoelectrochemical imaging of such a surface the localized temperature rise due to a focused laser spot is the dominant factor. An increase in the temperature may, in principle, induce a current by altering any or all of the structure of the electrical double layer,[14-18] the standard electrode potential,[19,20] the diffusion rate of electroactive species,[21-24] and rate of electron transfer.[25]

The purpose of this paper is to explore further the origin of the photothermal response at the gold/electrolyte interface. The spatial distribution of the photoinduced currents at a gold disc electrode were investigated both in the presence and absence of ferrocyanide over a wide potential range, providing important new information into the layers formed during the oxidation of gold.

* Abstract published in *Advance ACS Abstracts*, March 15, 1994.

(1) Vazquez, L.; Rodriguez, J. M. G.; Herrero, J. G.; Baro, A. M.; Garcia, N.; Canullo, J. C.; Arvia, A. J. *Surf. Sci.* **1987**, *181*, 98–106.
(2) Bard, A. J.; Denault, G.; Lee, C. M.; Mandler, D.; Wipf, D. O. *Acc. Chem. Res.* **1990**, *23*, 357–363.
(3) Lillard, R. S.; Moran, P. J.; Issacs, H. S. *J. Electrochem. Soc.* **1992**, *139*, 1007–1012.
(4) Cohn, R. F.; Wagner, J. W.; Kruger, J. *J. Electrochem. Soc.* **1988**, *135*, 1033–1034.
(5) Kozlowski, M.; Smyrl, W. H.; Atanasoska, L. J.; Atanasoska, R. *Electrochim. Acta* **1989**, *34*, 1763–1768.
(6) Peat, R.; Kucernak, A. R. J.; Williams, D. E.; Peter, L. M. *Semicond. Sci. Tech.* **1990**, *5*, 914–917.
(7) (a) Williams, D. E.; Kucernak, A. R. J.; Peat, R. *Electrochim. Acta* **1993**, *38*, 57–69, and 71–78. (b) Williams, D. E.; Kucernak, A. R. J.; Peat, R. *Faraday Discuss.* **1992**, *94*, 149–170.
(8) Hutton, R. S.; Williams, D. E. *J. Chem. Soc., Faraday Trans.* **1994**, *90*, 345–347.
(9) Kucernak, A. R.; Peat, R.; Williams, D. E. *J. Electrochem. Soc.* **1992**, *138*, 2337–2340.
(10) Hutton, R. S.; Williams, D. E. *Electrochim. Acta*, in press.
(11) (a) Peat, R.; Riley, A.; Williams, D. E. *J. Electrochem. Soc.* **1989**, *136*, 3352–3355. Peat, R.; Kucernak, A. R.; Williams, D. E. *Faraday Discuss.* **1992**, *94*, 369–385. (c) Peat, R.; Kucernak, A. R.; Williams, D. E. *Electrochim. Acta* **1992**, *37*, 933–942.
(12) Sass, J. K.; Gerischer, H. In *Photoemission and Electronic Properties of Surfaces*; Feuerbacher, B., Ed.; Wiley: New York, 1978; Chapter 16.
(13) Garcia, E.; Bard, A. J. *Chem. Phys. Lett.* **1985**, *120*, 437–440.
(14) Benderskii, V. A.; Vehlicho, G. I. *J. Electroanal. Chem.* **1982**, *140*, 1–22.
(15) Benderskii, V. A.; Vehlicho, G. I.; Kreitus, I. V. *J. Electroanal. Chem.* **1884**, *181*, 1–20.
(16) Barker, G. C.; Fowles, P.; Stringer, B. *Trans. Faraday Soc.* **1970**, *66*, 1509–1519.
(17) Barker, G. C. *Electrochim. Acta* **1968**, *13*, 1221–1244.
(18) Barker, G. C. *Ber. Bersunges. Phys. Chem.* **1971**, *75*, 728–736.
(19) Hutton, R. S.; Bond, A. M.; Colton, R.; Harvey, J., manuscript in preparation.
(20) Weaver, M. J. *J. Phys. Chem.* **1979**, *83*, 1748–1757.
(21) Miller, B. *J. Electrochem. Soc.* **1983**, *130*, 1639–1640.
(22) Valdes, J. L.; Miller, B. *J. Phys. Chem.* **1988**, *92*, 4483–4490.
(23) Valdes, J. L.; Miller, B. *J. Electrochem. Soc.* **1988**, *135*, 2223–2231.
(24) Valdes, J. L.; Miller, B. *J. Phys. Chem.* **1988**, *92*, 525–532.
(25) Curtiss, L. A.; Halley, J. W.; Hautman, J.; Haung, N. C.; Nagy, Z.; Rhee, Y. J.; Yonco, R. M. *J. Electrochem. Soc.* **1991**, *138*, 2032–2041.

0002-7863/94/1516-3453$04.50/0

Experimental Section

The principles of scanning laser photoelectrochemical microscopy (SCALPEM) have been described in detail elsewhere.[7] In this study a Bio-Rad Microscience Ltd. MRC 600 confocal laser microscope was used, modified to obtain variable linescan speeds. A focused light spot from an argon ion laser (514 nm) is rastered over the surface of an electrode using mirrors. Light returning from the specimen as a result of specular reflection is passed back through the microscope objective lens and monitored with a photomultiplier tube, to obtain an optical image of the electrode surface. Localized current perturbations for each beam position are accumulated and saved in a framestore to obtain a grey scale image (0–256). If the background current is stationary, then the perturbations are directly related to the influence of the impinging laser beam.

Experiments were performed in a conventional three electrode cell under potentiostatic control, the output of which was dc coupled through a preamplifier and offset to match the input range of the framestore. The image contrast therefore represents variations in current due to the movement of the laser spot across the surface. For each image the laser was scanned from left to right with variable velocity, 0.2–60 cm s^{-1}, the beam position was held for 0.06 s, and then the next line was scanned. Since the current changes induced by the laser were small in the system under study here (≈1 nA), measurements were signal averaged over multiple frames.

Working electrodes were made by encasing gold wire in epoxy resin and then polishing to a mirror finish with 30, 10, 3, 1, and 0.3 μm alumina powder water slurries. Analytical grade chemicals were used throughout with triply distilled water. Potentials were measured relative to a saturated calomel electrode (SCE).

Results and Discussion

The interaction of a focused light beam at a metallic electrode surface may in principle give rise to a variety of effects. However, it has been demonstrated previously[8] the dominant photoinduced current observed during the electrooxidation of ferrocyanide at gold is due to a thermally induced change in the rate of electron-transfer kinetics (termed the thermokinetic response). Presuming such a mechanism, the current changes observed during a photothermal electrochemical microscopy experiment can be deduced. Assuming a simple form for the local current density at constant potential

$$i = i_1 \exp[\Delta E_a/(RT)] \quad (1)$$

where ΔE_a denotes the activation energy for the electron-transfer reaction, the photothermal current change for a laser spot of area a, is simply given by

$$\delta I = (\delta T) i a \delta E_a/(RT^2) \quad (2)$$

Image contrast is therefore expected to arise from spatial variations in the dark current density, activation energy, and temperature change, the latter originating from spatial variations of the absorption coefficient of the light. Contrast might be observed around the edge of the electrode as a consequence of the difference in the thermal conductivity of the mounting and the electrode materials, further modified if there should be any flaws in the mounting with the electrode. Importantly **no** response should be observed where the reaction is controlled by mass transport since the activation energy for diffusion is small. Furthermore, when image spatial variations are due to kinetic control, the current variations induced should be proportional to the local dark current density and should therefore decrease with decreasing current density.[8]

Figure 1 shows a SCALPEM image obtained of a gold disc electrode in contact with 5 mmol dm^{-3} $K_4Fe(CN)_6$ (0.1 mol dm^{-3} K_2HPO_4 and 0.1 mol dm^{-3} KH_2PO_4) at a potential where the current is controlled by both electron-transfer kinetics and diffusion. Inspection of Figure 1 indicates that the photothermal image comprises several distinct features, the origins of which

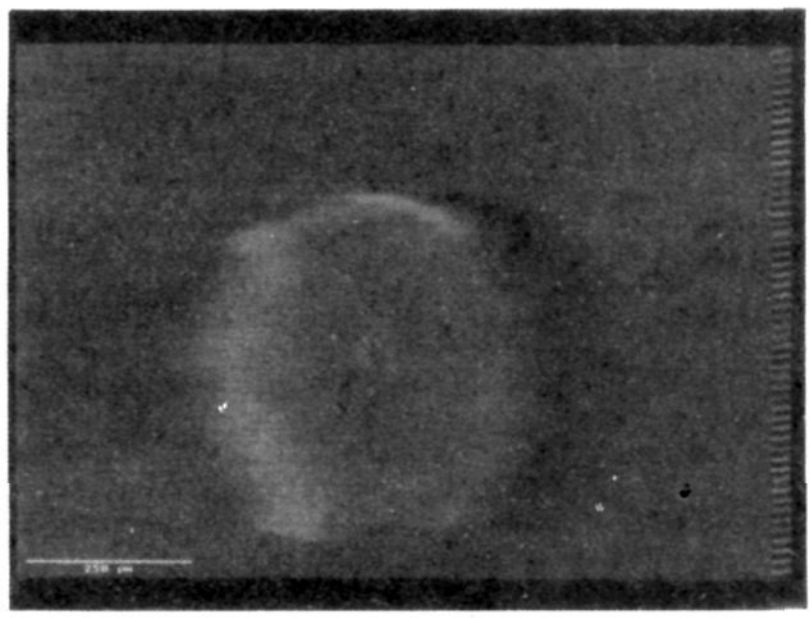

Figure 1. SCALPEM image of 5 mmol dm^{-3} $K_4Fe(CN)_6$ (0.1 K_2HPO_4 + 0.1 KH_2PO_4 mol dm^{-3}) at a gold electrode: pixel size 1.5 μm, image 767 × 512 pixels, grey scale 0–256 corresponds to $\delta i \approx 10$ nA, beam velocity 5.8 cm s^{-1}, beam diameter 4 μm, average of 50 frames, potential +200 mV vs SCE, scale bar 250 μm.

were investigated by systematically changing the electrode potential, ferrocyanide concentration, and laser spot characteristics.[8]

The primary SCALPEM response consisted of an annulus overlaying the electrode edge. The origin of this contrast may be rationalized by considering the reaction distribution at a disc electrode for a quasireversible reaction below the limiting current.[26,27] At the electrode center the rate-determining step is diffusion (semiinfinite planar), and consequently no photothermal response is observed. At the electrode edge faster radial diffusion is dominant, the reaction is kinetically controlled, and an easily detectable photothermal response is observed.

Figure 1 indicates several other image features in addition to this primary contrast. Local areas of activity (hotspots) are visible around the electrode edge, a feature that has been attributed to enhanced diffusion at submicrometer surface asperities, although both these and the primary contrast might be attributed to temperature variations across the edge of the specimen which are modified by the effect of heat transfer across the boundary between specimen and mounting. Transient phenomena are also evident, which result in blurring and shadowing of the image, the source of these being attributed to transient relaxation of the electrode temperature and of the local diffusion field.[8]

Analysis of the electrode potential dependence of images indicates as expected, at higher potentials, where diffusion control is dominant, the total photothermal response decreases. However, above 375 mV vs SCE the total photothermal response was found to increase again. It was proposed[8] that this effect may be due to the occurrence of additional reaction occurring in parallel with ferrocyanide oxidation, such as the oxidation of gold.

In order to investigate the influence of gold oxidation, images were recorded first with only the supporting electrolyte (0.1 M K_2HPO_4 + 0.1 M KH_2PO_4). Gold electrodes were pretreated by cycling the potential between –0.6 and 1.2 V vs SCE (20 mV s^{-1}) until a stationary voltammogram was obtained. Prior to each experiment the potential was held at an oxide free potential for several minutes (0 V vs SCE). Figure 2 shows a series of images recorded at a variety of dc potentials. Images were acquired with a long linescan time (20 ms/line) in order to increase image resolution. Such an approach lowers the laser spot velocity thereby increasing the local temperature rise and, in this instance, reducing the influence of transient effects.

(26) Baker, D. R.; Verbrugge, M. W. *J. Electrochem. Soc.* **1990**, *137*, 1832–1842.
(27) Verbrugge, M. W.; Baker, D. R. *J. Phys. Chem.* **1992**, *96*, 4572–4580.

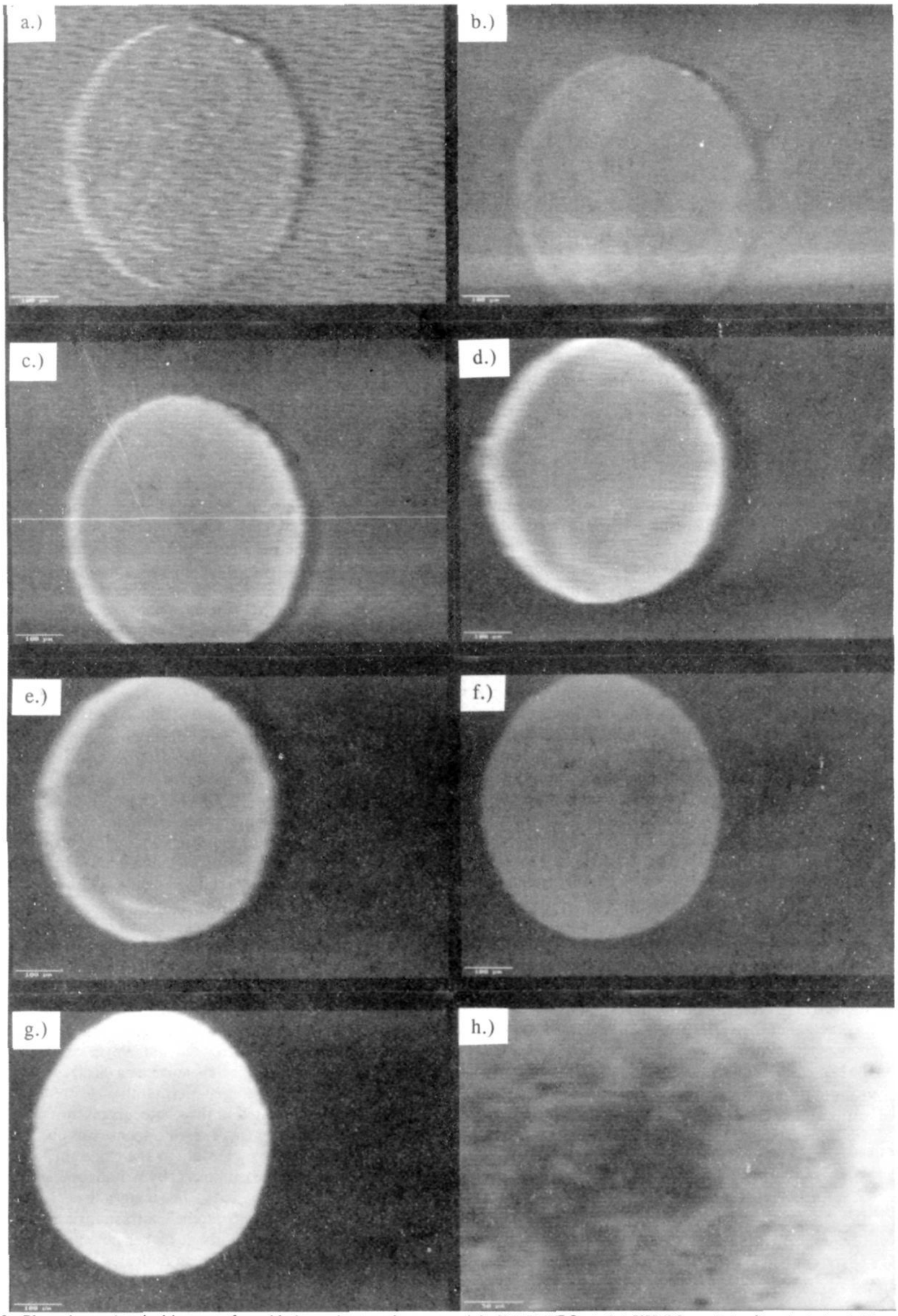

Figure 2. Photoelectrochemical images of a gold electrode at various potentials (0.1 K_2HPO_4 + 0.1 KH_2PO_4 mol dm^{-3}): pixel size 1.17 μm, image 767 × 512 pixels, grey scale 0–256 number in brackets/nA, beam velocity 4.5 cm s^{-1}, beam diameter 2 μm, potentials V vs SCE (a) 0.2 (9.0), (b) 0.7 (15.3), (c) 0.8 (16.7), (d) 0.9 (24.7), (e) 1.1 (100), (f) 1.2 (200), (g) 1.4 (200), and (h) 1.4, scale bar (a–g) 100 μm, (h) 50 μm.

Figure 2a indicates that even at +200 mV vs SCE a small response is obtained in a region where the surface is oxide free. The origin of this effect can be identified with thermal effects on the double layer capacitance,[28] akin to observations made by Benderskii and Barker[14–18] at mercury. The photothermal

(28) Hutton, R. S.; Williams, D. E., manuscript in preparation.

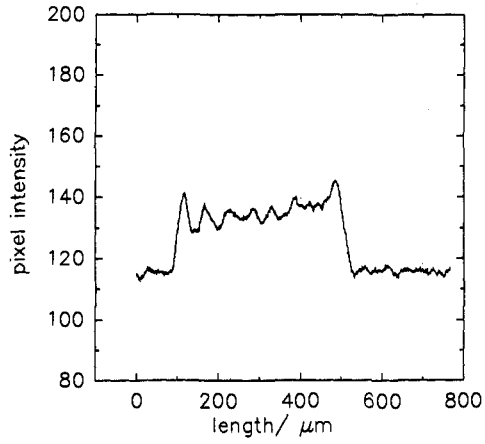

Figure 3. Plot of pixel intensity versus distance, showing enhanced photothermal current at the electrode edge and the sloping base due gradual heating of the electrode.

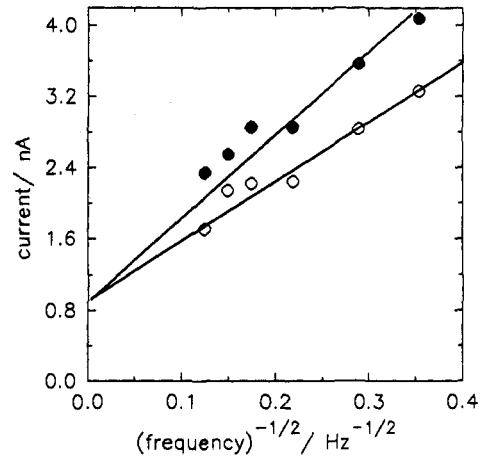

Figure 4. Plot of the average pixel intensity at the electrode center (○) and edge (●) versus modulation frequency$^{-1/2}$ obtained from lock-in photoelectrochemical images: potential 1.0 V vs SCE, gold in 0.1 K_2HPO_4 + 0.1 KH_2PO_4 mol dm^{-3}, beam velocity 0.39 cm s^{-1}, beam diameter 2 μm.

response was found to decrease in magnitude with increasing potential. However at approximately +700 mV vs SCE the photothermal current intensified (Figure 2b). A relatively even signal was observed across the electrode surface, with only minor contrast variations, which by comparison with the corresponding optical image are assigned to changes in the electrode reflectivity. Several hotspots are apparent around the electrode edge with associated shadowing. Figure 3 shows a plot of the pixel intensity across the region marked in Figure 2c, which clearly demonstrates the enhanced response around the electrode edge, some contrast over the electrode surface, and also shows that the average signal increased in magnitude as the laser spot traversed the surface: this is a characteristic of the photothermal effect for an irreversible electrode reaction (here gold electrooxidation) and may be attributed to the gradual heating of the whole electrode surface as the laser spot traverses it. In this case the contrast enhancement around the electrode edge is due to a larger temperature change there (see later Discussion). Whilst the two image features mentioned above can clearly be attributed to the photothermal effect, the origin of the current variations across the electrode surface is less clear. The observed contrast might partially in principle be due to photohole emission: however, this mechanism may be discounted since it is a inefficient process[29,30] (quantum efficiency approx. 10^{-9}) and only expected with illumination in the deep ultraviolet.[31] An anodic photocurrent generated within a gold oxide layer is however a possible source of image contrast. Within this potential region, which is below the onset of regular oxide formation (1.11 V vs SCE[32]), an incipient oxide exists which covers only a fraction of the surface.[32-36] It has been shown by a variety of optical techniques[37-39] that the incipient oxide absorbs strongly in the UV–visible and gives rise to a small photocurrent.[32]

Owing to the different time responses of the photocurrents generated within anodic oxides[40] and the thermally induced current,[14] which decreases with diminishing illumination time, examination of the intensity modulated frequency response enabled the thermokinetic current contribution toward the total photocurrent to be set apart. In this experiment, the focused light spot was intensity modulated by an optoacoustic modulator, and a lock-in amplifier was then used to extract that component of the current modulated at the same frequency of the illumination. Thus by scanning the laser beam slowly, the output of the lock-in amplifier represents the local surface photocurrent response. Figure 4 shows a plot of the average pixel intensity at the electrode center and edge, versus $1/(f)^{1/2}$, where f is the modulation frequency. Figure 4 indicates that a linear relationship between current and (frequency)$^{-1/2}$ is obtained, characteristic of a thermal response,[14] which was larger at the electrode edge. Extrapolation of the data in Figure 4 indicates that at higher modulation frequencies the current does not fall to zero, thus demonstrating a fraction of the response arises from photocurrent generated within the oxide layer. Inspection of pixel intensity across the electrode center as a function of modulation frequency, consequently, confirmed contrast is associated with photocurrents generated within the oxide layer.

Upon increasing the potential the total photoinduced current was found to increase dramatically. At approximately 1.2 V vs SCE the enhanced response around the electrode edge, characteristic of the photothermal effect, was found to disappear, resulting in a relatively even response across the electrode. Significantly, the potential at which this happened corresponds to that for formation of a regular monolayer oxide (≈1.1 V vs SCE). Figure 5 shows the dependence on electrode potential of the pixel intensity averaged across the electrode center, a parameter closely related to the photocurrent measured during nonlocalized experiments. A small response was observed below 1.1 V vs SCE, rapidly increasing as the oxide thickened, in an analogous manner to measurements by Watanabe and Gerischer[32] at much lower light intensities. The images show, superimposed upon this average behavior, some contrast variation across the electrode surface, particularly at higher potentials. Inspection of the images shown in Figure 2h indicates that contrast arises from two sources: increased photoactivity due to multiple reflections associated with scratches and regions of inactivity. The photoinactive regions appear to change with potential: at low potentials they are large and give rise to a mottled pattern across the surface, whereas at higher potentials they appear as ≈10 μm diameter dark dots randomly distributed across the surface. The most likely interpretation is that the image is

(29) Murakoshi, K.; Uosaki, K. *Phys. Rev. B Cond. Mat.* **1993**, *47*, 2278–2288.
(30) Plieth, W. J.; Rieger, H. J.; Aljaafgolze, K. *J. Electroanal. Chem.* **1987**, *228*, 283–292.
(31) Watanabe, T.; Gerischer, H. *J. Electroanal. Chem.* **1981**, *122*, 73–91.
(32) Watanabe, T.; Gerischer, H. *J. Electroanal. Chem.* **1981**, *117*, 185–200.
(33) Burke, L. D.; O'Sullivan, J. F. *Electrochim. Acta* **1992**, *37*, 585–594.
(34) Burke, L. D.; Lyons, M. E. G. In *Modern Aspects of Electrochemistry*; Bard, A. J., Ed.; 1986; Vol. 18, Chapter 4, pp 169–248.
(35) Nguyen Van Huong, C.; Hinnen, C.; Lecoeur, J. *J. Electroanal. Chem.* **1980**, *106*, 185.
(36) Manne, S.; Massie, J.; Elings, V. B.; Hansma, P. K.; Gewirth, A. A. *J. Vac. Sci. Tech.* **1991**, *B9*, 950–954.
(37) Kim, Y. T.; Collins, R. W.; Vedam, K. *Surf. Sci.* **1990**, *233*, 341–350.
(38) Dohrmann, J. K.; Sander, U.; Strehblow, H. H. *Z. Physik. Chem. Neue Folge* **1983**, *134*, 41–55.
(39) Masuda, H.; Fujishima, A.; Honda, K. *Bull. Chem. Soc. Jpn.* **1980**, *53*, 1542–1546.
(40) Peat, R.; Peter, L. M. *J. Electroanal. Chem.* **1987**, *228*, 351–364.

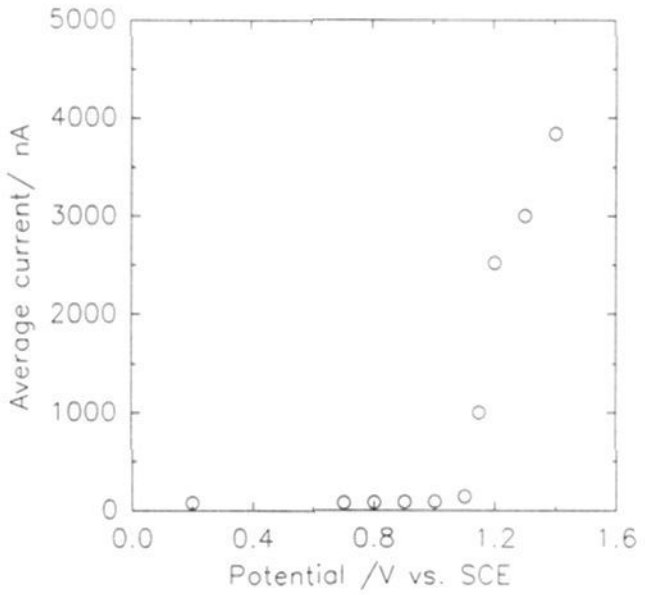

Figure 5. Plot of the mean pixel intensity obtained from photoelectrochemical images versus electrode potential for gold in 0.1 K_2HPO_4 + 0.1 KH_2PO_4 mol dm^{-3}.

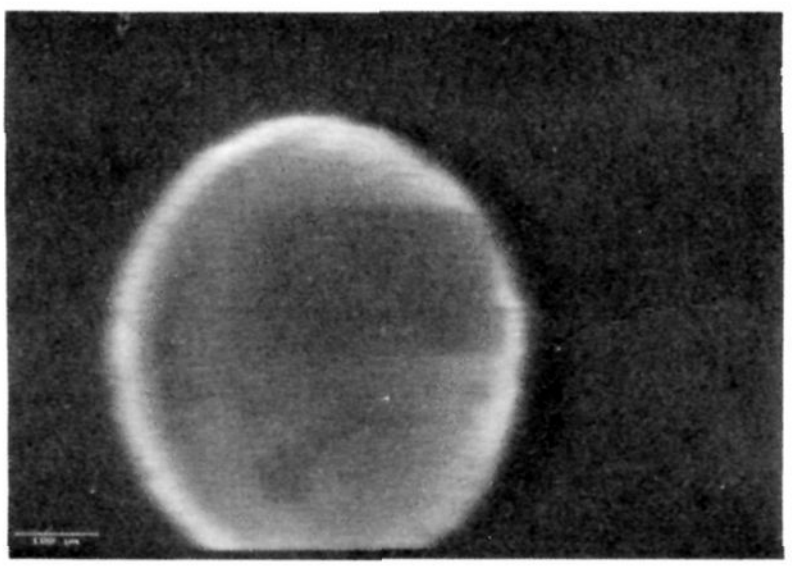

Figure 6. Photoelectrochemical image of a gold electrode at +900 mV vs SCE (0.1 K_2HPO_4 + 0.1 KH_2PO_4 mol dm^{-3}) showing the persistent effect of previously zooming in onto a part of the electrode surface: pixel size 1.17 μm, grey scale 0–256 corresponds to $\delta i \approx 25$ nA, beam velocity 4.5 cm s^{-1}, beam diameter 2 μm, scale bar 100 μm.

displaying the spatial variation of surface recombination rate of photoexcited charge carriers.

It was noted that if the laser was scanned over a smaller area this had a drastic effect on the subsequent images. Figure 6 shows a photoelectrochemical image acquired after such an exposure of a part of the surface: superimposed upon part of the previously described response is a dark rectangle where the laser has "deactivated" the surface. This result is interpreted as due to a photoinduced aging or reconstruction of the oxide layer, as observed by Watanabe and Gerischer[32] at potentials above 1.15 V vs SCE in 0.2 mol dm^{-3} $NaClO_4$. These authors concluded that the magnitude of the photocurrent obtained at gold is determined not only by the oxide thickness but also by its state at the time of measurement, films undergoing a slow transformation in the dark, and a rapid change under illumination.

In the present work, we found that the photodeactivation of the surface by intense illumination was only possible at potentials greater than 800 mV vs SCE. The deactivation of the surface was found to be a considerably irreversible process: further prolonged oxidation or reduction below the formal gold oxide reduction peak failed to remove the inactive rectangle, and intense illumination had no effect on the oxide reduction curve. Surprisingly, in order to remove the inactive layer it was necessary to reduce the potential into the hydrogen evolution region. It is concluded that a stable species which inhibits electron transfer is formed by the intense illumination of an oxidized gold electrode. A possible candidate is a hydrous oxide species, such as $Au_2(OH)_9^{3-}$ which is known to inhibit both oxidation and reduction processes on gold. It is noted that similar, extremely stable species have been proposed controversially on platinum.[41]

In order to investigate further the origin of photoeffects and to enhance the contribution due to the photothermal effect, photoelectrochemical images were recorded in the presence of 1 mmol dm^{-3} potassium ferrocyanide (0.1 M K_2HPO_4 + 0.1 M KH_2PO_4). Figure 7 shows a series of images recorded under identical conditions to the data in Figure 2, at a variety of dc potentials. At low potentials, in the absence of surface oxide, the response was dominated by the thermokinetic response due to the oxidation of ferrocyanide at surface asperities. As the potential was increased, only small changes in images were observed, because under the conditions chosen (low Fe(II) concentration) the reaction is mainly diffusion controlled.[8] As the potential was increased further, islands of photoactivity became apparent (at $\approx$+500 mV vs SCE), which slowly grew in size, with increasing potential. In view of the later discussion we remark here that these islands represent areas where the change in current induced by the illumination was largest, and they do not necessarily correspond to regions where the dark current density was largest. The current change associated with the islands was found to be approximately constant below $\approx$1.0 V vs SCE, drastically increasing at higher potentials, in an identical manner to that found in the absence of ferrocyanide (cf. Figure 5). The islands continued to develop with increasing potential, up to the point where current transients associated with oxygen bubble formation limit image acquisition, when the oxide layer is several monolayers thick.[37]

The photoactive islands were found to be stable. Reducing the potential to +200 mV vs SCE for several minutes had no effect on the island pattern, which could only be removed by prolonged hydrogen evolution followed by subsequent image acquisition at anodic potentials, thus indicating the pattern is due to an immobile stable surface species and not to the underlying metal microstructure.

The mechanism for the enhancement of image contrast in the presence of Fe(II) is considered. Firstly, holes formed by the photoexcitation in the oxide layer and trapped at the interface could oxidize Fe(II) in solution, giving a photocurrent increase. This mechanism has been utilized to image surface states on anodic TiO_2.[42] Secondly, the thermokinetic contrast could reappear: Figure 8 shows difference voltammograms between the current in the presence and that in the absence of ferrocyanide, illustrating that the current due to electrooxidation of ferrocyanide drops when an oxide is nucleated on gold. This inhibition can obviously be considered as due to the presence of a complete layer of oxide over the surface.[43,44] More controversially it has been proposed that electron transfer is inhibited by species present at submonolayer coverage before the nucleation of the film.[45,46]

Our argument is that the image contrast in the presence of Fe(II) arises as a consequence of the photothermal effect, because the inhibition of electron transfer is not uniform across the surface. The interpretation is that on inhibited areas the current would be limited by electron-transfer kinetics, with a relatively large activation energy. The current change resulting from illumination would therefore be largest on the inhibited areas.

(41) Burke, L. D.; Roche, M. B. C. *J. Electroanal. Chem.* **1984**, *164*, 315–334.
(42) McMillan, C. S.; Sukamto, J. P. H.; Smyrl, W. H. *Faraday Discussion* **1992**, *94*, 63–75.
(43) Kuhn, A. T.; Randle, T. H. *J. Chem. Soc., Faraday Trans.* **1985**, *81*, 403–419.
(44) Damjanovic, A.; Birss, V. I.; Boudreaux, D. S. *J. Electrochem. Soc.* **1991**, *138*, 2549–2555.
(45) Burke, L. D.; O'Sullivan, J. F.; O'Dwyer, K. J.; Scannel, R. A.; Ahern, M. J. G.; McCarthy, M. M. *J. Electrochem. Soc.* **1990**, *137*, 2476–2481.
(46) Oesch, U. *Electrochim. Acta* **1983**, *28*, 1247–1253.

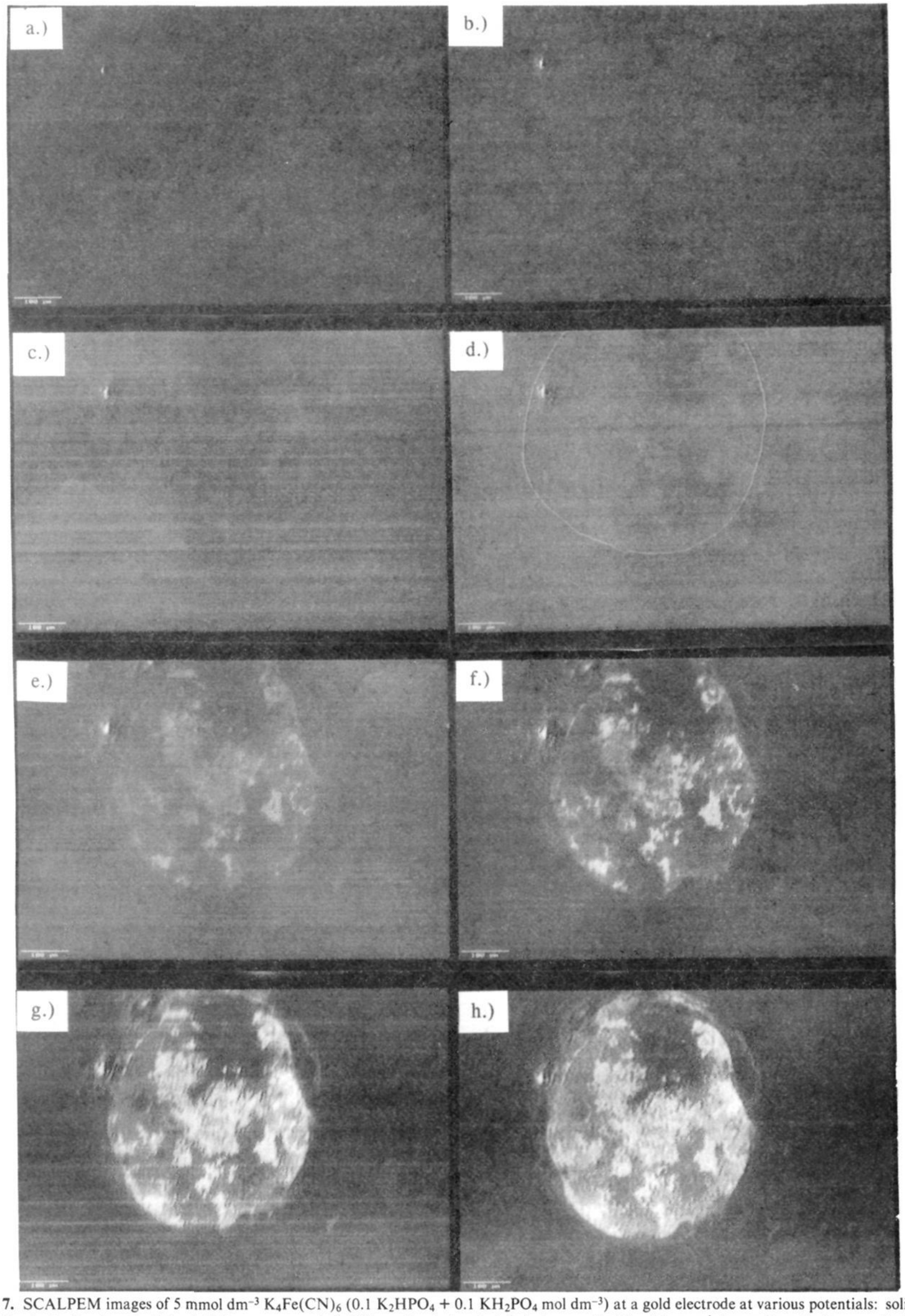

Figure 7. SCALPEM images of 5 mmol dm^{-3} $K_4Fe(CN)_6$ (0.1 K_2HPO_4 + 0.1 KH_2PO_4 mol dm^{-3}) at a gold electrode at various potentials: solid line highlights electrode edge, pixel size 1.175 μm, grey scale 0–256 number in brackets/nA, beam velocities 4.5 cm s^{-1}, beam diameter 2 μm, potential/V vs SCE (a) 0.25 (20), (b) 0.5 (20), (c) 0.6 (20), (d) 0.7 (20), (e) 0.8 (20), (f) 0.9 (20), (g) 1.0 (20), and (h) 1.1 (50), scale bar 100 μm.

Conclusions

Scanning laser photoelectrochemical microscopy has been shown to be a powerful tool for investigating electrochemical heterogeneity in situ. The present investigation has illustrated and part differentiated a number of sources of image contrast. Thus, the photoexcitation of charge carriers in the anodic oxide

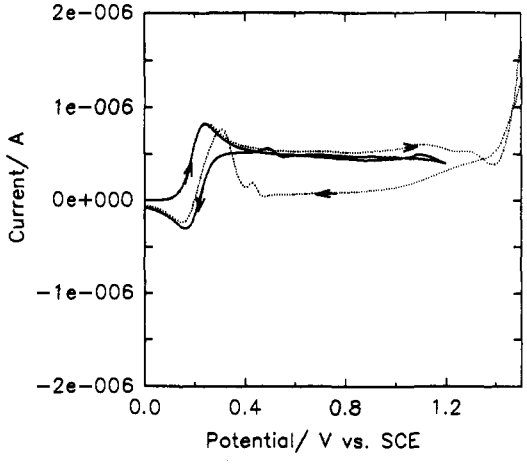

Figure 8. Cyclic difference voltammograms, of current in the presence and in the absence of ferrocyanide, demonstrating that oxide nucleation above 1.2 V vs SCE inhibits ferrocyanide oxidation: scan rate 10 mV s^{-1} 5 mmol dm^{-3} $K_4Fe(CN)_6$ (0.1 K_2HPO_4 + 0.1 KH_2PO_4 mol dm^{-3}).

on gold gave a small photocurrent contrast attributable to variations in surface recombination rate; the photothermal effect on gold electrooxidation (an irreversible process) gave contrast attributable to variation in the photoinduced temperature change; the photothermal effect on ferrocyanide oxidation on clean gold (a quasireversible reaction) shows activation energy contrast; the photothermal effect on ferrocyanide oxidation on oxidized gold showed a spectacular contrast, attributed again to activation energy variations, with some effects due to variable temperature changes around the electrode edge. The origin of this chemical heterogeneity on oxidized gold was investigated by examining the influence of electrode potential and pretreatment, indicating that the inactivity is due to a chemical species formed below regular monolayer oxide formation. Significantly this incipient oxide was found to be stable. It influenced image contrast up to oxygen evolution and could only be removed by prolonged hydrogen evolution. An apparently related phenomenon was observed under intense illumination, which resulted in a deactivation of the surface.

Acknowledgment. This work was funded by the Science and Engineering Research Council. The authors are grateful to Bio-Rad Microscience Ltd. for technical assistance.